Online in color, print in grayscale unless the author(s) contribute to the costs.
These are not the final page numbers! ↘↘

Chemie
Ingenieur
Technik

Research Article

1

Melt Emulsions: Influence of the Cooling Procedure on Crystallization and Recrystallization of Emulsion Droplets and their Influence on Dispersion Viscosity upon Storage

Jasmin Reiner*, Tran T. Ly, Lingyue Liu, and Heike P. Karbstein

Dedicated to Prof. Dr. Thomas Hirth on the occasion of his 60th birthday

Emulsions with crystalline dispersed phase are widely used formulations in life sciences. Unfortunately, these products often are unstable resulting in changes of their rheological behavior. These changes could be linked to shape transformations of crystallized droplets, depending on the cooling rate in their production and temperature of storage. In a thermo-optical method, shape changes were investigated in a broad range of constant cooling rates or cooling rate ramps close to industrial processes. Cooling at slow to moderate cooling rates ($0.1–50\,\mathrm{K\,min^{-1}}$), as found in typical stirred vessel tanks, induced self-shaping of droplets during crystallization, which resulted in platelet-like particles and fibers, deviating greatly from the formerly spherical shape. In contrast, fast cooling as found in heat exchangers resulted in mostly spherical shapes less prone to recrystallization-induced instabilities.

1 Introduction

Emulsions with crystalline dispersed phase are widely used in the pharmaceutical, chemical and life science industry [1–4]. They are used as high-performance lubricants, release agents for demolding or as delivery systems for the targeted and controlled release of bioactive compounds [5–7]. Due to the viscoelastic behavior of the encapsulating material, these systems are usually produced via a two-step melt emulsification process: first, the dispersed phase is emulsified at temperatures above the melting range using rotor-stator systems or high-pressure homogenization. The second step comprises the cooling process, where the emulsion is transferred into a crystalline dispersion [8–10].

In contrast to bulk crystallization, droplets in a collective show stochastic and individual crystallization behavior differing from droplet to droplet [11, 12]. During cooling, they can remain as supercooled liquid or solidified amorphous particle or in different crystalline structures. These differences to bulk crystallization occur due to significant differences in the formation of nuclei because of the extremely small volume of the lipid phase within the emulsified droplets [8, 13]. In bulk lipids, mainly heterogeneous nucleation caused by the presence of catalytic impurities takes place [14], whereas the formation of nuclei in emulsi-

fied lipid droplets often occurs due to homogeneous nucleation [15, 16]. Once stable nuclei are formed, they grow into crystals. The crystallization behavior of the droplets greatly depends on process parameters and the formulation, in particular on the droplet size, additives, surfactants, cooling rate, supercooling and external forces [12, 17–22]. If the hydrophobic compound crystallizes within a droplet, the oil-water interface acts as a physical boundary to crystal growth. Ideally, by choosing suitable process parameters and dispersion ingredients, each droplet crystallizes in its original size and shape [17, 22–24]. Nevertheless, solid triacylglycerol particles with nanometer size are known to quickly change their shape from spherical to ellipsoid or other shapes due to polymorphic transitions, or even solidify in ellipsoid shapes when crystallizing directly into β-polymorph [25–27].

Jasmin Reiner, Tran T. Ly, Lingyue Liu,
Prof. Dr.-Ing. Heike P. Karbstein
jasmin.reiner@kit.edu
Karlsruhe Institute of Technology, Institute of Process Engineering in Life Sciences, Food Process Engineering, Gotthard-Franz-Straße 3, 76131 Karlsruhe, Germany.

Online in color, print in grayscale unless the author(s) contribute to the costs.
✓✓ **These are not the final page numbers!**

2

Research Article

Chemie
Ingenieur
Technik

Recently, it was also shown that liquid hydrocarbon droplets can undergo several morphological transitions during cooling, spontaneously breaking their shape symmetry multiple times and then freezing into solid non-spherical particles [28–30]. The particle shapes differ from octahedral, polygonal platelets, O-shapes to fibers. The deformation is induced by the crystallization of the surfactant molecules, which then triggers the formation of the rotator phase of the alkanes [28, 30–33]. The rotator phase is an intermediate phase alkanes form during cooling between the isotropic liquid phase and the fully ordered, solid crystalline phase [34–37]. These intermediate phases get their name because the molecules have long-range positional order in the three-dimensional space, but exhibit significant freedom in their molecular rotation. Multilayers of this plastic rotator phase at the drop surface provide sufficient bending energy to initiate drop-shape transformations [28, 30]. In order to induce the drop-shape transformation, the capillary pressure and interfacial tension have to be overcome. This is achieved due to the high bending constant of the multilayer of alkane molecules, assembled into the rotator phase [28]. Surfactants initiating this process require a long and saturated surfactant tail (comparable length to alkane molecule) and a not too large headgroup [30]. This suggests that a dense adsorption layer on the drop surface freezes before the interior of the droplet crystallizes [32]. As for droplet crystallization in general, the cooling rate and initial droplet size also strongly influence the drop shape evolution during cooling [29]. The drop-shape evolution generally follows the scheme, which was introduced and adapted by [28, 30] for hexadecane emulsion drops shown in Fig. 1. The shape changes in the beginning differ dependent on the applied cooling rate with an examined maximum of $4\,\mathrm{K\,min^{-1}}$. The process was statistical and additionally depends on the drop size and surfactant type. At a given droplet size between $10–20\,\mu m$, slower cooling increased the probability of triangular platelets, whereas less tetragonal plates were formed.

The size and shape of crystalline particles within a dispersion can have an influence on its physicochemical properties like mouthfeel and rheology [25] and on its physical stability, like aggregation or creaming [34, 35]. Crystalline dispersions are thermodynamically unstable systems and therefore underlie instability mechanisms like creaming, flocculation, Ostwald ripening, phase inversion and (partial) coalescence [36–38]. Additionally, recrystallization and polymorphic transitions may negatively influence the dispersion characteristics during storage and transport [39–42]. These instability mechanisms are well researched. However, manufacturers of crystalline dispersions still often struggle in naming factors for their products that lead to instability. The behavior of fat crystals under industrially relevant ("real world") conditions has been less studied so far [41]. Instability mechanisms of relevance are thus less known. To the best of our knowledge, a comprehensive investigation on the influence of drop deformation during cooling of melt emulsions on the dispersion stability has not been reported yet. This study concentrates on drop deformation during crystallization under defined and under industry-oriented process conditions (emulsification: rotor-stator-machine & cooling: stirring tank, heat exchanger). Particle shapes and recrystallization effects during storage are correlated with changes in dispersion characteristics upon storage.

2 Material and Methods

2.1 Materials

All materials were commercially available and used as purchased without further purification or processing. Octadecane (purity 99 %, melting point at 29 °C) and polyoxyethylene (20) stearyl ether (Brij® S20) were purchased from Sigma-Aldrich® (St. Louis, MO, USA). Water was purified using a MircoPure™ Water purification system (Waltham, MA, USA).

2.2 Emulsion Preparation

All emulsions consisted of octadecane as disperse phase and purified water as continuous phase. Brij® S20 was used as surfactant. First, the surfactant was dissolved in tempered purified water at 40 °C. Afterwards, octadecane was added to the surfactant solution and molten under continuous
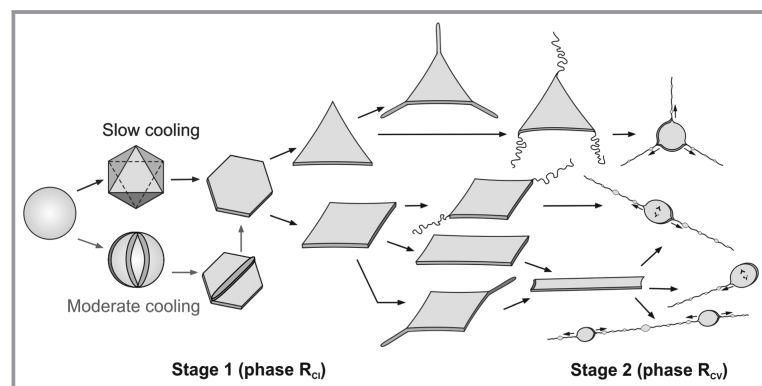
Figure 1. General evolution scheme for the drop-shape transformations upon cooling of alkane drops stabilized by surfactants introduced and adapted by [28, 30].

Online in color, print in grayscale unless the author(s) contribute to the costs.
These are not the final page numbers! ↘↘

Chemie
Ingenieur
Technik

Research Article

3

stirring for at least 15 min at 40 °C. Then, octadecane was homogenized at different volumetric specific energies (E_V) to prepare emulsions with different mean droplet diameter and varying fraction of disperse phase:

1) 10 wt % octadecane and 2 wt % Brij® S20: First, a coarse emulsion was produced using a tooth-rim dispersing machine at 3.3 m s^{-1} tangential speed (5000 rpm, 13 mm outer diameter of the rotating part) for 1 min. To produce the fine emulsion, E_V was applied with a colloid mill dispersing machine (IKA® magic Lab, Staufen im Breisgau, Germany) at 23.7 m s^{-1} tangential speed (15 000 rpm) for 10 min or at 15.8 m s^{-1} tangential speed (10 000 rpm) for 5 min.

2) 1 wt % octadecane and 1 wt % Brij® S20: E_V was applied using a tooth-rim dispersing machine (IKA® T25 digital, ULTRA-TURRAX®, Staufen im Breisgau, Germany) at 2.2 m s^{-1} tangential speed (3200 rpm, 13 mm outer diameter of the rotating part) for 10 min in a glass vessel of 25 mm inner diameter.

During homogenization, the temperature was always kept 10 K above the melting point of octadecane to prevent premature crystallization. Afterwards samples were taken for storage tests (10 wt % dispersions) and thermo-optical analysis (cryo-polarizing microscopy, only 1 wt % octadecane emulsions). After emulsion preparation, all emulsions were characterized using a laser diffraction particle size analyzer (HORIBA LA-940, Retsch Technology, Haan, Germany) in a stirred fraction cell. The refractive index used for octadecane was 1.439 + 0.000i. Emulsions were strongly diluted and measured three times at room temperature after crystallization. The measuring range of the instrument is between 0.01 and 3000 μm for round particles due to data analysis using a combination of laser diffraction and Mie scattering theory. Emulsions for storage tests (1) had monomodal size distributions with a Sauter mean diameter of approx. 1.5 μm and a span of 5.5. Emulsions for thermo-optical analysis (2) had a Sauter mean diameter of approx. 22 μm with a span of 1.

2.3 Storage Tests

Recrystallization of particles during storage and their influence on dispersion stability was determined over a period of three months. Samples were taken at regular intervals for optical analysis and particle size measurements.

2.3.1 Characterization of Morphology and Recrystallization Behavior during Storage

After melt emulsification and crystallization, optical analysis on dispersions was performed using the polarizing light microscope. Suspensions consisting of 10 wt % octadecane were strongly diluted prior to analysis. One drop of diluted sample was pipetted on a microscope object slide and then covered with a microscope cover slip. All dispersions were characterized at room temperature. This measurement allowed the determination of crystallinity and particle morphology directly after preparation, as well as the detection of changes during storage.

2.3.2 Rheological Characterization of Stored Dispersions

The rheological behavior of octadecane dispersions was characterized over the storage period of three months. Oscillatory measurements were conducted in the linear viscoelastic range in order to preserve the dispersion structure and to prevent particle breakage during measurements. The rheological properties of dispersions were determined using a Physica MCR 301 rotational Rheometer (Anton Paar, Graz, Austria). All measurements were conducted with a double gap geometry DG26.7.

Amplitude sweeps were conducted to determine the linear viscoelastic range of the dispersions. On this basis, an amplitude of 0.01 % was chosen for the frequency sweeps. Frequency sweeps were conducted at angular frequencies ranging from 100 to 0.1 rad s^{-1}. The frequency was increased logarithmically, and 22 points were recorded per decade.

All samples were produced at least three times prior to their rheological measurement. As particle size varied complex viscosities at 1 rad s^{-1} were stated as related values ($\eta^\star/\eta^\star_{t0}$) over storage time.

2.4 Characterization of Drop Shape Evolution and Crystallization Behavior

The thermo-optical observation of the drop-shape evolution and the crystallization behavior of 1 wt % octadecane-in-water emulsions during cooling was examined using a polarizing microscope (Eclipse LV100ND, Nikon, Shinagawa, Tokyo, Japan) equipped with an optically accessible temperature-controlled stage (LTS 420, Linkam Scientific, Tadworth, UK). Sample preparation for microscopic analysis took place according to Abramov et al. [11]. The temperature of the emulsion and the object slides was kept constant at 10 K above the melting point of octadecane. This ensured that no crystallization occurred prior to thermo-optical analysis.

To investigate the crystallization behavior and drop-shape evolution during cooling, constant cooling rates of 0.2, 1.0 and 20.0 and 50.0 K min^{-1} were applied with each cooling representing slow, moderate and fast cooling, respectively. Additionally, cooling rate ramps were applied imitating industrial cooling processes in stirring tanks, where defined cooling cannot be realized. These ramps were chosen according to temperature-time curves obtained for cooling at 22 °C (room temperature, RT), at 6 °C (refrigerator, RF) and at 0 °C (ice bath, IB). Industrial heat exchangers with cooling rates > 25 K s^{-1} were mimicked by giving a

Online in color, print in grayscale unless the author(s) contribute to the costs.
✓✓ These are not the final page numbers!

4

Research Article

Chemie
Ingenieur
Technik

small product sample (1 mL) to liquid nitrogen (LN) representing extreme fast cooling. Each cooling rate or ramp was investigated in triplicate while picture sequences were automatically taken during the procedure.

2.5 Statistical Analysis

All samples were prepared three times independently. All tests were performed at least three times if not stated otherwise. Uncertainty was calculated using Microsoft Excel 2019 or Origin 2018 and expressed as standard deviation.

3 Results and Discussion

3.1 Recrystallization of Dispersions during Storage

The influence of particle recrystallization and instability mechanisms during storage on dispersion characteristics was determined for 10 wt % octadecane dispersions over a storage period of three months. Fig. 2 displays the related complex viscosity ($\eta*/\eta*_{t0}$) at 1 rad s^{-1} directly after crystallization and over storage at 6 °C (RF) and 22 °C (RT). In all samples, the complex viscosity decreases over time. In samples stored at 6 °C ($\Delta T = 23$ K below the melting temperature of octadecane), the decrease in complex viscosity occurred gradually over time. Crystalline dispersions stored at 22 °C ($\Delta T = 7$ K) exhibited a significant drop in complex viscosity already after one month of storage. This is in contrast to triglyceride solid lipid nanoparticle suspensions, where extensive gelation due to aggregation is often observed over storage [25, 39].

Polarized microscopic images of the initial crystalline dispersion and after one and three months of storage at 6 °C and 22 °C are depicted in Fig. 3. Initially, a mixture of long and some shorter fibers were present after crystallization. Particles were fully crystalline prior to storage, according to the supercooling of 23 K applied. After storage, shorter and
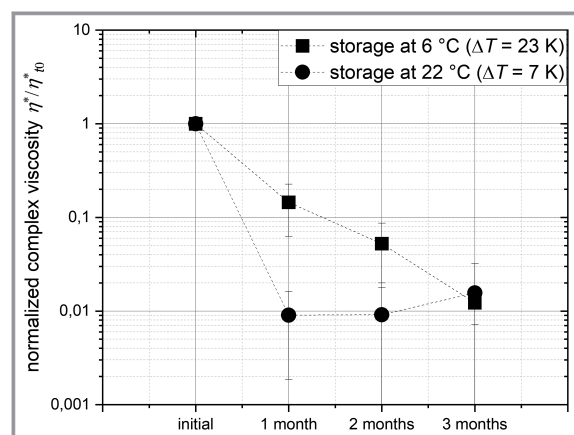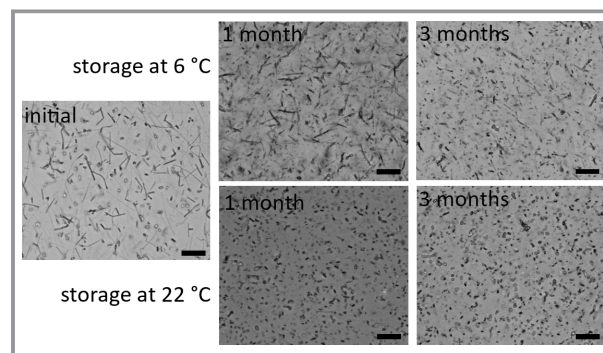
Figure 3. Microscopic images of 10 wt % octadecane dispersions after preparation (initial) and after storage of 1 month and 3 months at 6 °C and 22 °C. Length of the scale bar is 25 μm.

rounder structures can be observed. While storage at 6 °C ($\Delta T = 23$ K) resulted mainly in shorter fibers after three months, mainly round shapes were found for storage at 22 °C ($\Delta T = 7$ K).

In [43] it was shown that recrystallization rates can increase up to twenty times when the storage temperature is raised from –20 °C to –5 °C. In the case of ice crystals, smoothing and rounding of particle surfaces occurs due to iso-mass rounding effects by Ostwald ripening.

Recrystallization due to migration and accretion (as found, e.g., for ice crystals in ice cream) typically results in ice crystal growth and broadening of the size distribution [44, 45]. In the investigated crystalline dispersions, particles' shape rounded but the particles did not obviously grow within the three months of storage time.

The alteration in particle morphology due to recrystallization correlates well with the drop of complex viscosity during storage. Disintegration of fibers and recrystallization to smoother, more rounded shapes lead to the overall decrease of complex viscosity. It was shown that for glass fibers at constant dispersed phase volume, the longer the fibers are, the higher the complex viscosity is [46]. The drop in viscosity after one month of 22 °C storage correlates well with the faster particle recrystallization due to the less pronounced supercooling compared with 6 °C storage.

Different particle morphologies cannot only be the result of recrystallization. Varying process conditions may also lead to dissimilar initial morphologies. Fig. 4 depicts exemplary microscopic images of the dispersions after three different cooling procedures: cooling at room temperature (RT), in the refrigerator (RF) and in an ice bath (IB). With decreasing cooling rate, the amount and length of fibers increased. In the ice bath, short cylindrical as well as triangular particles were obtained. The slower cooling rate in the RF and RT resulted mainly in the formation of long fibers.

Figure 2. Normalized viscosity ($\eta*/\eta*_{t0}$) over storage time for storage at 6 °C (RF, $\Delta T = 23$ K) and 22 °C (RT, $\Delta T = 7$ K)

Chemie Ingenieur Technik

Research Article

Online in color, print in grayscale unless the author(s) contribute to the costs.
These are not the final page numbers! ↘↘

5
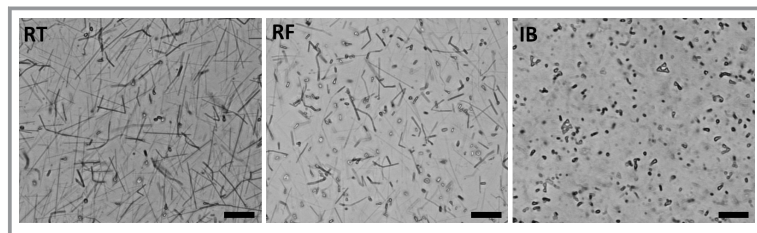
Figure 4. Microscopic images of 10 wt % octadecane dispersions after crystallization under three different conditions: cooling at room temperature (RT), cooling in the refrigerator (RF) and cooling in an ice bath (IB). Length of the scale bar is 25 µm.

3.2 Controlling the Particle Shape via the Cooling Process

In order to get a better understanding of the droplet self-shaping during cooling, we used our thermo-optical method [11] to investigate the drop-shape transformation and thus resulting particle shape under different process conditions, namely the cooling rate. For the optical investigations, 1 wt % emulsions were used to save the additional dilution step. Additionally, initial droplet sizes were larger than for storage tests to better visualize the deformations. First, different constant cooling rates were applied to adjust the method for these self-shaping effects and investigate the drop deformation at high cooling rates. Then, we applied different temperature-time curves with varying cooling rates to control the particle shape. These cooling rate ramps were chosen according to data obtained by the different cooling methods applied to the 10 wt % octadecane dispersions.

3.2.1 Controlled Crystallization under Constant Cooling Rates

Polarized light microscopy images of 1 wt % octadecane dispersions stabilized with Brij® S20 obtained for defined cooling rates between 0.2 and 50 K min^{-1} are shown in Fig. 5. The drop shaping mainly follows the general evolution scheme obtained upon cooling of hexadecane introduced by [28, 30]. With increasing cooling rate, the self-shaping of droplets was less pronounced and lower aspect ratios were obtained.

At 0.2 K min^{-1} (Fig. 5a) large hexagonal platelets with a big hole in the center and some very thin fibers are formed, as described by [28–30] for cooling rates of 0.01–4 K min^{-1}. 1 K min^{-1} (Fig. 5b) resulted mainly in smaller, but also flat hexagonal platelets with a hole in the center, or an even thinner crystal layer in the center. Some thicker hexagons were also obtained. However, at 20 K min^{-1} the drop-shape evolution did not follow the evolution scheme for fast cooling rates given in [28, 30], but rather the one proposed for slow cooling. Hexagons were formed that flattened within seconds, sometimes showing protrusions. Hexagonal platelets with a hole in their center, full hexagons or football

shapes were finally formed (see Fig. 5c). At 50 K min^{-1}, particles started to slightly deform before full crystallization. The majority of particles found were hexagons appearing as balls with irregular edges. Besides, a few platelets can be monitored that originated from the smallest initial droplets. This corresponds to findings of [28, 30], reporting different shapes for the same cooling rate as result of differences in the initial droplet sizes.

In Tab. 1, the onset temperature of droplet self-shaping, the onset temperature of crystalli-
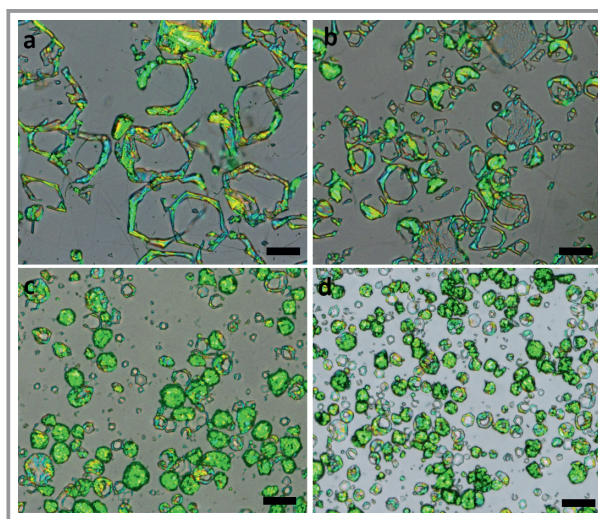
Figure 5. Microscopic images of 1 wt % octadecane dispersions after full crystallization with cooling rates of a) 0.2, b) 1.0, c) 20.0 and d) 50.0 K min^{-1}. Length of the scale bar is 50 µm.

Table 1. Onset temperature range of self-shaping ($\theta_{\text{self-shaping}}$), onset temperature of crystallization (θ_{cr}) and temperature of total crystallization ($\theta_{\text{cr,total}}$) of octadecane dispersions for different cooling rates.

Cooling rate [K min^{-1}]	Onset $\theta_{\text{self-shaping}}$ [°C]	Onset θ_{cr} [°C]	$\theta_{\text{cr,total}}$ [°C]
0.2	28.5 ± 0.5	26.7 ± 0.1	23.5 ± 0.5
1.0	27.4 ± 0.2	26.2 ± 0.1	22.9 ± 0.5
20	25.9 ± 0.8	24.5 ± 0.6	15.7 ± 0.6

zation and the temperature of full droplet crystallization are listed for the cooling rates 0.1, 1.0 and 20.0 K min^{-1}. At 50.0 K min^{-1}, transitions happened too quickly to be stated. Temperatures are stated as mean values including standard deviations. With increasing cooling rate, a higher supercooling was needed for the initiation of self-shaping. At a cooling rate of 0.2 K min^{-1} self-shaping started around the melting temperature of octadecane, whereas for the other cooling rates a supercooling up to approx. 3.5 K was needed. The temperature of full particle crystallization also

Online in color, print in grayscale unless the author(s) contribute to the costs.
✓✓ **These are not the final page numbers!**

6

Research Article

Chemie
Ingenieur
Technik

decreased with increasing cooling rate, which is in accordance with crystallization of spherical droplets [4, 11, 18, 21].

As a dense adsorption layer of surfactant on the drop surface freezing before the interior of the droplet is required for self-shaping [32], lower supercooling is needed with slower cooling rates. Surfactant molecules then have more time to adsorb and arrange at the interface. This also applies for crystallization, where molecules have time to find the most favorable conformation. As soon as sufficient supercooling is achieved, molecules are ready to crystallize. At fast cooling, crystallization is delayed because molecules need time to take the shape of the right conformation. Even a cooling rate of $50\,K\,min^{-1}$ was not fast enough to fully prevent molecule arrangement and thus self-shaping.

3.2.2 Controlled Crystallization Applying Cooling Rate Ramps

Cooling of emulsions on a laboratory or industrial scale mostly does not occur at constant cooling rates, except for heat exchangers. Mostly, small or large volumes are slowly cooled under stirring at room temperatures or with cooled double jackets. Corresponding temperature profiles obtained by the different cooling methods applied to the 10 wt % octadecane dispersions are depicted in Fig. 6 for different temperatures of the cooling media. These profiles were replicated in the optical method by calculating the respective cooling rate for each time step and implementing it as a stepwise cooling program. The target temperature was different for each cooling method due to the different temperatures prevailing. When the sample was cooled at room temperature, it could not get colder than the existing room temperature. Overall, cooling in an ice bath (IB) represents a fast cooling method, cooling at room temperature (RT) and in the refrigerator (RF) represent moderate and slow cooling. Nevertheless, in all processes cooling takes place faster in the beginning and to the end the curves flatten. In the refrigerator cooling rates did range between 0.5 and $0.2\,K\,min^{-1}$ in the relevant temperature range where self-shaping and crystallization took place. In these temperature ranges cooling at room temperature was even slower with rates between 0.01 and $0.1\,K\,min^{-1}$.

Microscopic images of dispersions obtained after the respective temperature time ramps are depicted in Fig. 7. Overall, slow cooling (RT imitation) led to the formation of very long and thin fibers as well as triangular or hexagonal platelets. The thin fibers are visible in the background of the image. At the end of the cooling process, some droplets remained supercooled liquid droplets. The imitation of refrigerator cooling (RF) mainly resulted in hexagonal platelets with a hole in the center, as well as some fibers in the background. A few platelets were obtained by the ice bath (IB) cooling profile, whereas a lot of particles
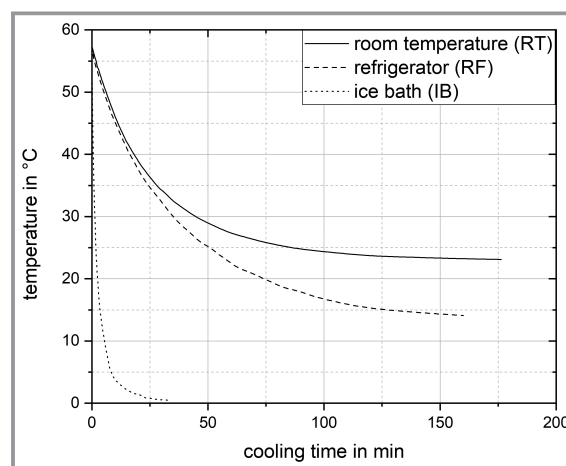
Figure 6. Temperature time curves obtained for different cooling processes representing slow (RT), moderate (RF) and fast cooling (IB) with varying cooling rates over time.

obtained were in hexagonal shape. These results show that self-shaping is also found in cooling profiles typical for industrial processes. The resulting shape mainly depends on the cooling rate during the critical temperature range. The critical temperature range differs depending on the oil surfactant combination, initial droplet size and cooling rate [28–30]. For the model system, the resulting particle shape was particularly dependent on the cooling rate during the relevant temperature range at supercooling (ΔT) of 2–5 K where self-shaping and crystallization occurred. In this temperature range, cooling rates in the IB, RF and at RT were $10\,K\,min^{-1}$, $0.4\,K\,min^{-1}$ and 0.1–$0.01\,K\,min^{-1}$, respectively.

In Tab. 2, the onset temperature of droplet self-shaping, the onset temperature of crystallization and the temperature of full crystallization for the different cooling processes are stated. Self-shaping and crystallization onset temperatures in ice bath cooled samples were similar to fast cooling ($20\,K\,min^{-1}$) with constant cooling rates. The temperature range for total emulsion crystallization imitating ice bath cooling was larger than under constant fast cooling. Here, the varying cooling rates during the process lead to a bigger variance between experiments. The three different temperature ranges for RF imitation were similar to the ones obtained under constant cooling with $1.0\,K\,min^{-1}$. Emulsions cooled with the RT imitation profile did not fully crystallize
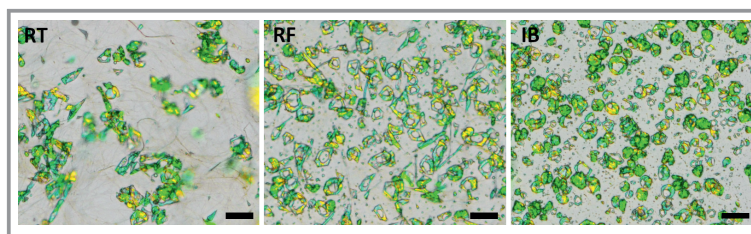
Figure 7. Microscopic images of 1 wt % octadecane dispersions after crystallization with three different cooling rate ramps. Length of the scale bar is 50 μm.

Online in color, print in grayscale unless the author(s) contribute to the costs.
These are not the final page numbers! ↘

Chemie
Ingenieur
Technik   **Research Article**   7

Table 2. Onset temperature ranges of self-shaping ($\theta_{\text{self-shaping}}$), onset temperature of crystallization (θ_{cr}) and temperature of total crystallization ($\theta_{\text{cr,total}}$) of octadecane dispersions for three different cooling profiles.

Profile imitating cooling process at/in	Onset $\theta_{\text{self-shaping}}$ [°C]	Onset θ_{cr} [°C]	$\theta_{\text{cr,total}}$ [°C]
room temperature	27.1 ± 0.4	26.3 ± 0.1	< RT
refrigerator	26.5 ± 0.5	25.9 ± 1.0	22.8 ± 0.3
ice bath	25.0 ± 0.3	23.8 ± 0.2	16.7 ± 2.1

under the investigated parameter. The majority of deformed droplets crystallized, but a few liquid droplets were still observed at the final temperature (23 °C). Hence, supercooling was not sufficient to induce full droplet crystallization even with these very slow cooling rates. These supercooled liquid droplets will either stay liquid or may crystalize gradually over storage [21].

In industrial processes using heat exchangers, cooling rates up to $25\,\text{K}\,\text{s}^{-1}$ can be achieved. These cooling rates cannot be applied by the cooling stage in the experimental setup used. Thus, a small amount of sample (1 mL) was cooled in liquid nitrogen to imitate very fast cooling by heat exchangers. The resulting particle shape for two different initial droplet sizes can be seen in Fig. 8. In both dispersions, the majority of particles crystallized in a fully spherical shape. In sample b, where the majority of droplets was between 3–5 μm, particles exhibit a rough and uneven surface. Using liquid nitrogen for cooling, time was not sufficient in order to initiate surfactant crystallization and the formation of the intermediate rotator phase before droplet crystallization.
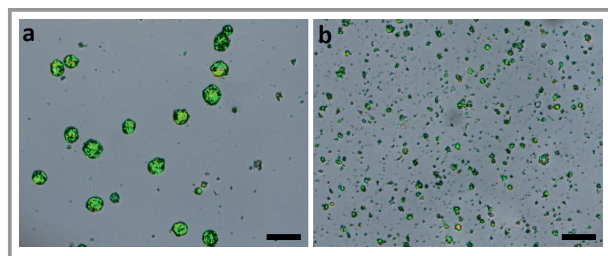
Figure 8. Microscopic images of 1 wt % octadecane dispersions after full crystallization by cooling in liquid nitrogen. Length of the scale bar is 50 μm. a) Energy input (E_V) = 2.2 m s^{-1}, b) E_V = 6.8 m s^{-1}.

4 Conclusion

Drop-shape transformations of octadecane droplets stabilized with Brij® S20 were observed for different cooling methods varying from very slow ($0.01\,\text{K}\,\text{min}^{-1}$) to moderate ($1\,\text{K}\,\text{min}^{-1}$) and fast ($20\,\text{K}\,\text{min}^{-1}$) cooling rates. Especially the formation of long fibers was observed. During storage, these long fibers disappeared and smoothing of particle surfaces and edges by recrystallization was observed, known

from ice crystal recrystallization [44]. Partial coalescence and aggregation, as reported for triacylglycerol dispersions [25, 39], hardly took place and was negligible compared to particle rounding and disintegration of long fibers due to recrystallization. Both, the disintegration and smoothing of particles occurred faster at storage temperatures closer to the melting temperature (lower supercooling) of the dispersed phase. These morphological changes in particle shape did affect the overall dispersion characteristics. We were able to correlate the recrystallization and disintegration of fibers with a significant decrease in complex viscosity for all samples. A gradual decrease in complex viscosity at cold storage (high supercooling) was observed, whereas the value dropped fast for samples stored at room temperature (low supercooling). In contrast to theoretical expectations (e.g., [24]), we could not detect extensive aggregation of fibers during storage of particles shapes with high surface area. However, the significant drop in complex viscosity may later lead to an increased creaming rate, which again increases the probability of agglomeration, which will further alter product characteristics or even lead to the total loss of required product functions.

Self-shaping of droplets in melt emulsions due to formation of a rotator phase by induced surfactant crystallization were observed using a thermo-optical method under constant cooling with cooling rates up to $50\,\text{K}\,\text{min}^{-1}$. The extent of self-shaping decreased with increasing cooling rate, corresponding to results reported in literature for cooling rates up to $4\,\text{K}\,\text{min}^{-1}$ [28]. The self-shaping was also found for cooling ramps simulating stirred tank cooling in industrial processes to different final temperatures and thus supercooling of the dispersed phase. The resulting particle shape was particularly dependent on the cooling rate during the relevant temperature range at supercooling of ΔT 2–5 K, where self-shaping and crystallization occurred. Drop-shape transformations could only be prevented by very fast cooling in liquid nitrogen, as was shown for droplet sizes between 3–30 μm. At this very fast cooling rate, particles did not form fibers, but spherical shapes, being significantly less prone to disintegration or rounding during storage. If desired, the drop-shape transformations may thus be prevented by very rapid cooling in heat exchangers.

Our results clearly show that crystalline dispersions with particle shapes deviating from the spherical shape exhibit strong recrystallization during storage resulting in a significant loss of product viscosity. Such shapes will always be found, if the surfactant crystallization at the droplet/continuous phase interface triggers the formation of the intermediate rotator phase of the disperse phase [28–30]. The thermo-optical method used in this study is ideally suited for investigating these processes and possible influencing factors.

Online in color, print in grayscale unless the author(s) contribute to the costs.
✓✓ These are not the final page numbers!
8
Research Article

Chemie
Ingenieur
Technik

Symbols used

ΔT	[K]	supercooling
θ	[°C]	temperature

Abbreviations

IB	ice bath
RF	refrigerator
RT	room temperature

References

[1] R. H. Müller, R. Shegokar, C. M. Keck, *Curr. Drug Discovery Technol.* **2011**, *8 (3)*, 207–227. DOI: https://doi.org/10.2174/157016311796799062

[2] R. H. Müller, R. D. Petersen, A. Hommoss, J. Pardeike, *Adv. Drug Delivery Rev.* **2007**, *59 (6)*, 522–530. DOI: https://doi.org/10.1016/j.addr.2007.04.012

[3] J. Pardeike, A. Hommoss, R. H. Müller, *Int. J. Pharm.* **2009**, *366 (1–2)*, 170–184. DOI: https://doi.org/10.1016/j.ijpharm.2008.10.003

[4] D. J. McClements, *Adv. Colloid Interface Sci.* **2012**, *174*, 1–30. DOI: https://doi.org/10.1016/j.cis.2012.03.002

[5] J. Weiss, E. A. Decker, D. J. McClements, K. Kristbergsson, T. Helgason, T. Awad, *Food Biophys.* **2008**, *3 (2)*, 146–154. DOI: https://doi.org/10.1007/s11483-008-9065-8

[6] R. H. Müller, K. Mäder, S. Gohla, *Eur. J. Pharm. Biopharm.* **2000**, *50 (1)*, 161–177. DOI: https://doi.org/10.1016/S0939-6411(00)00087-4

[7] P. E. Romero, J. Arribas-Barrios, O. Rodriguez-Alabanda, R. González-Merino, G. Guerrero-Vaca, *CIRP J. Manuf. Sci. Technol.* **2021**, *32*, 396–404. DOI: https://doi.org/10.1016/j.cirpj.2021.01.019

[8] P. Walstra, *Physical Chemistry of Foods*, Food science and technology, Vol. 121, Marcel Dekker, New York **2003**.

[9] K. Köhler, A. Hensel, M. Kraut, H. P. Schuchmann, *Particuology* **2011**, *9 (5)*, 506–509. DOI: https://doi.org/10.1016/j.partic.2011.03.009

[10] S. Fanselow, S. E. Emamjomeh, K.-E. Wirth, J. Schmidt, W. Peukert, *Chem. Eng. Sci.* **2016**, *141*, 282–292. DOI: https://doi.org/10.1016/j.ces.2015.11.019

[11] S. Abramov, P. Ruppik, H. Schuchmann, *Processes* **2016**, *4 (4)*, 25. DOI: https://doi.org/10.3390/pr4030025

[12] S. Abramov, A. Berndt, K. Georgieva, P. Ruppik, H. P. Schuchmann, *Colloids Surf., A* **2017**, *529*, 513–522. DOI: https://doi.org/10.1016/j.colsurfa.2017.06.029

[13] J. N. Coupland, *Curr. Opin. Colloid Interface Sci.* **2002**, *7 (5–6)*, 445–450. DOI: https://doi.org/10.1016/S1359-0294(02)00080-8

[14] C. Himawan, V. M. Starov, A. G. F. Stapley, *Adv. Colloid Interface Sci.* **2006**, *122 (1–3)*, 3–33. DOI: https://doi.org/10.1016/j.cis.2006.06.016

[15] Z. Kožíšek, K. Sato, S. Ueno, P. Demo, *J. Chem. Phys.* **2011**, *134 (9)*, 94508. DOI: https://doi.org/10.1063/1.3559453

[16] E. Günther, T. Schmid, H. Mehling, S. Hiebler, L. Huang, *Int. J. Refrig.* **2010**, *33 (8)*, 1605–1611. DOI: https://doi.org/10.1016/j.ijrefrig.2010.07.022

[17] D. J. McClements, S. R. Dungan, J. B. German, C. Simoneau, J. E. Kinsella, *J. Food Sci.* **1993**, *58 (5)*, 1148–1151. DOI: https://doi.org/10.1111/j.1365-2621.1993.tb06135.x

[18] M. Tippetts, S. Martini, *Food Res. Int.* **2009**, *42 (7)*, 847–855. DOI: https://doi.org/10.1016/j.foodres.2009.03.009

[19] İ. Gülseren, J. N. Coupland, *J. Am. Oil Chem. Soc.* **2007**, *84 (7)*, 621–629. DOI: https://doi.org/10.1007/s11746-007-1093-x

[20] S. Abramov, A. Ahammou, H. P. Karbstein, *Chem. Eng. Technol.* **2018**, *41 (4)*, 768–775. DOI: https://doi.org/10.1002/ceat.201700586

[21] S. Abramov, K. Shah, L. Weißenstein, H. Karbstein, *Processes* **2018**, *6 (1)*, 6. DOI: https://doi.org/10.3390/pr6010006

[22] H. Bunjes, M. H. J. Koch, K. Westesen, *J. Pharm. Sci.* **2003**, *92 (7)*, 1509–1520. DOI: https://doi.org/10.1002/jps.10413

[23] F. Kesisoglou, S. Panmai, Y. Wu, *Adv. Drug Delivery Rev.* **2007**, *59 (7)*, 631–644. DOI: https://doi.org/10.1016/j.addr.2007.05.003

[24] H. Bunjes, M. H. J. Koch, K. Westesen, *Langmuir* **2000**, *16 (12)*, 5234–5241. DOI: https://doi.org/10.1021/la990856l

[25] T. Helgason, T. S. Awad, K. Kristbergsson, D. J. McClements, J. Weiss, *J. Am. Oil Chem. Soc.* **2008**, *85 (6)*, 501–511. DOI: https://doi.org/10.1007/s11746-008-1219-9

[26] K. Jores, W. Mehnert, M. Drechsler, H. Bunjes, C. Johann, K. Mäder, *J. Controlled Release* **2004**, *95 (2)*, 217–227. DOI: https://doi.org/10.1016/j.jconrel.2003.11.012

[27] H. Bunjes, F. Steiniger, W. Richter, *Langmuir* **2007**, *23 (7)*, 4005–4011. DOI: https://doi.org/10.1021/la062904p

[28] N. Denkov, S. Tcholakova, I. Lesov, D. Cholakova, S. K. Smoukov, *Nature* **2015**, *528 (7582)*, 392. DOI: https://doi.org/10.1038/nature16189

[29] N. Denkov, D. Cholakova, S. Tcholakova, S. K. Smoukov, *Langmuir* **2016**, *32 (31)*, 7985–7991. DOI: https://doi.org/10.1021/acs.langmuir.6b01626

[30] D. Cholakova, N. Denkov, S. Tcholakova, I. Lesov, S. K. Smoukov, *Adv. Colloid Interface Sci.* **2016**, *235*, 90–107. DOI: https://doi.org/10.1016/j.cis.2016.06.002

[31] Z. Valkova, D. Cholakova, S. Tcholakova, N. Denkov, S. K. Smoukov, *Langmuir* **2017**, *33 (43)*, 12155–12170. DOI: https://doi.org/10.1021/acs.langmuir.7b02048

[32] D. Cholakova, N. Denkov, *Adv. Colloid Interface Sci.* **2019**, *269*, 7–42. DOI: https://doi.org/10.1016/j.cis.2019.04.001

[33] D. Cholakova, N. Denkov, S. Tcholakova, Z. Valkova, S. K. Smoukov, *Langmuir* **2019**, *35 (16)*, 5484–5495. DOI: https://doi.org/10.1021/acs.langmuir.8b02771

[34] K. Boode, C. Bisperink, P. Walstra, *Colloids Surf.* **1991**, *61*, 55–74. DOI: https://doi.org/10.1016/0166-6622(91)80299-4

[35] K. Boode, P. Walstra, *Colloids Surf., A* **1993**, *81*, 121–137. DOI: https://doi.org/10.1016/0927-7757(93)80239-B

[36] P. Walstra, in *Food emulsions and foams: Interfaces, interactions and stability*, Woodhead Publishing Series in Food Science, Technology and Nutrition, Vol. 16, Woodhead Publishing Ltd., Cambridge **1987**.

[37] S. A. Vanapalli, J. Palanuwech, J. N. Coupland, *Colloids Surf., A* **2002**, *204 (1–3)*, 227–237. DOI: https://doi.org/10.1016/S0927-7757(01)01135-9

[38] H. D. Goff, *J. Dairy Sci.* **1997**, *80 (10)*, 2620–2630. DOI: https://doi.org/10.3168/jds.S0022-0302(97)76219-2

[39] T. S. Awad, T. Helgason, K. Kristbergsson, E. A. Decker, J. Weiss, D. J. McClements, *Food Biophys.* **2008**, *3 (2)*, 155–162. DOI: https://doi.org/10.1007/s11483-008-9057-8

[40] A. G. F. Stapley, H. Tewkesbury, P. J. Fryer, *J. Am. Oil Chem. Soc.* **1999**, *76 (6)*, 677–685. DOI: https://doi.org/10.1007/s11746-999-0159-3

[41] D. Rousseau, *Food Res. Int.* **2000**, *33 (1)*, 3–14. DOI: https://doi.org/10.1016/S0963-9969(00)00017-X

[42] S. Ghosh, D. Rousseau, *Curr. Opin. Colloid Interface Sci.* **2011**, *16 (5)*, 421–431. DOI: https://doi.org/10.1016/j.cocis.2011.06.006

Online in color, print in grayscale unless the author(s) contribute to the costs.
These are not the final page numbers! ↘↘

Chemie Ingenieur Technik   **Research Article**   9

[43] D. P. Donhowe, R. W. Hartel, *Int. Dairy J.* **1996**, *6 (11–12)*, 1191–1208. DOI: https://doi.org/10.1016/S0958-6946(96)00029-5

[44] D. P. Donhowe, R. W. Hartel, *Int. Dairy J.* **1996**, *6 (11–12)*, 1209–1221. DOI: https://doi.org/10.1016/s0958-6946(96)00030-1

[45] R. Sutton, J. Bracey, *Dairy Ind. Int.* **1996**, *61 (2)*, 31–33.

[46] B. Hochstein, *Rheologie von Kugel- und Fasersuspensionen mit viskoelastischen Matrixflüssigkeiten*, Dissertation, Universität Karlsruhe **1997**.

Online in color, print in grayscale unless the author(s) contribute to the costs.
✓✓ These are not the final page numbers!
10   Research Article | Chemie Ingenieur Technik

Melt Emulsions: Influence of the Cooling Procedure on Crystallization and Recrystallization of Emulsion Droplets and their Influence on Dispersion Viscosity upon Storage

Jasmin Reiner*, Tran T. Ly, Lingyue Liu, Heike P. Karbstein

Research Article: Crystalline dispersions are often unstable resulting in changes of their rheological behavior. These changes can be linked to shape transformations of crystallized droplets and their recrystallization behavior during storage. The influence of cooling procedure on particle shape and crystallization of droplets is investigated and related with its influence on particle recrystallization and alterations of dispersion characteristics during storage. .... ■